JACS
JOURNAL OF THE AMERICAN CHEMICAL SOCIETY

ARTICLE

pubs.acs.org/JACS

A Fluorescent, Shape-Persistent Dendritic Host with Photoswitchable Guest Encapsulation and Intramolecular Energy Transfer

Thi-Thanh-Tam Nguyen, David Türp, Dapeng Wang, Belinda Nölscher, Frédéric Laquai, and Klaus Müllen*

Max-Planck-Institute for Polymer Research, Ackermannweg 10, D-55128 Mainz, Germany

Supporting Information

ABSTRACT: A fluorescent and photoresponsive host based on rigid polyphenylene dendrimers (PPDs) has been synthesized. The key building block for the divergent dendrimer buildup is a complex tetracyclone **12** containing azobenzenyl, pyridyl, and ethynyl entities. The rigidity of polyphenylenes is of crucial importance for a site-specific placement of different functions: eight azobenzene (AB) moieties into the rigid scaffold, a fluorescent perylenetetracarboxdiimide (PDI) into the core, and eight pyridin functions into the interior cavities. AB moieties of host−**1** undergo reversible cis−trans photoisomerization and are photostable, as confirmed by various techniques: UV−vis, ^{1}H NMR, size exclusion chromatography, and fluorescence correlation (FCS). In this system, AB moieties act as photoswitchable hinges and enable control over (i) molecular size, (ii) intramolecular energy transfer between AB and PDI, and (iii) encapsulation and release of guest molecules. The presence of PDI allows not only following the effect of cis−trans photoisomerization on molecular size with highly sensitive FCS but also monitoring the efficiency of the intramolecular energy transfer process (from AB to PDI) by time-resolved optical spectroscopy. Pyridyl functions were incorporated to facilitate guest uptake via hydrogen bonds between the host and guests. Also, we have demonstrated that the photoswitchability of the host can be utilized to actively encapsulate guest molecules into its interior cavities. This novel, light-driven encapsulation mechanism could enable the design of new drug delivery systems.

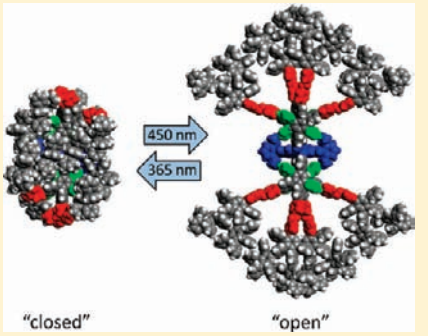

1. INTRODUCTION

Macromolecules that are responsive to an external stimulus in a controlled and reproducible manner have many potential applications.[1−14] They allow one to reversibly manipulate and change molecular properties such as shape, conformation, or polarity whenever desired.[13] Especially the cis−trans photoisomerization of azobenzene (AB) continues to attract tremendous interest since its discovery in the late 1930s.[15] Owing to its photostability and the substantial geometrical change accompanying cis−trans isomerization, AB has enabled the development of a variety of photoresponsive functional materials and devices, including smart polymers,[7,9] molecular machines,[10] and molecular switches.[8] There have been attempts to combine the conformational switchability of AB with the structural perfectness and multivalency of dendrimers.[16−24] Dendrimers define an active field of research because of their many unique properties,[25−35] which also make them preferential candidates for the use as hosts in advanced drug delivery systems.[36−41] Since then, the number of papers concerning dendritic host−guest systems has been continuing to increase. Vögtle et al. reported that the peripheral decoration of a polypropyleneamine dendrimer with 32 AB moieties enables changing the permeability of the dendritic shell toward guest molecules.[18] However, due to the flexibility of most types of dendrons, the conformational change of AB can only affect its close molecular environment. To achieve a pronounced photoinduced change of the overall dendritic shape and structure remains a challenging task.

It is known that polyphenylene dendrimers (PPDs)[42,43] are rigid and shape-persistent. These properties prevent them from collapsing and thus their interior voids are permanently maintained. In previous work of our group, AB was successfully used as a PPD core.[44] The resulting dendrimer exhibits a significant conformational change upon cis−trans photoisomerization. Thus, it was expected that the introduction of several AB moieties into specific sites of a rigid PPD scaffold would amplify the effect of size and shape change.

Here, we aim to design a photoswitchable dendritic host based on PPDs. The photoswitching should be driven by the cis−trans photoisomerization of ABs. The system should be able to both physically encapsulate guest molecules and release them by way of drastically changing its overall shape: a "closed" structure of the host would encapsulate guest molecules permanently until a change to an "open" structure would allow the release of guests from its interior (Figure 1).

The system presented herein should serve as an organosoluble model for investigating the effect of AB isomerization on the change of dendrimer shape and guest encapsulation/release as well as a model system for photoswitching of intramolecular energy transfer processes. Also, the proposed mechanism has implications for the design of new dendritic drug delivery systems. Usually, drugs are covalently linked to their hosts in order to

Received: March 11, 2011
Published: June 17, 2011

dx.doi.org/10.1021/ja2022398 | J. Am. Chem. Soc. 2011, 133, 11194–11204

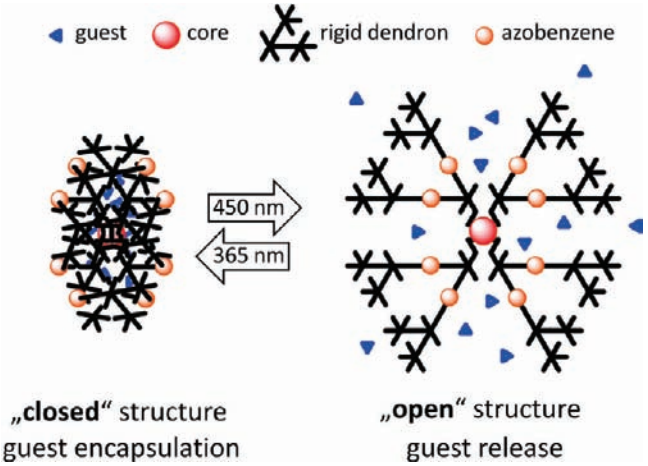

Figure 1. Proposed mechanism for the photoswitched encapsulation and release mechanism.

prevent premature drug leaching, while release is triggered by a bond-breaking stimulus (usually pH).[45] However, covalent linking requires a chemical modification of the drugs, and this may reduce their efficiency.[46] In contrast, our proposed mechanism of physical encapsulation could enable the delivery of nonlinked, unmodified, and active drugs while still preventing them from premature leaching.

We chose to employ a perylenetetracarboxydiimide (PDI) dye as a central fluororescent chromophore in our host model because of its outstanding stabilities and high fluorescence quantum yields[47−49] and the accumulated expertise of our group regarding the dendronization of bay functionalized PDIs with rigid polyphenylenes.[50]

Additionally, the highly fluorescent PDI in the core of the dendrimer is a very effective probe for intramolecular energy transfer processes, as the combination of AB in the scaffold and PDI in the dendrimer represents an energy transfer, i.e., donor−acceptor system. Intramolecular energy transfer in dendrimers has already been reported by us and others,[50−64] but the combination of a photoswitchable donor (AB) and a fluorescent acceptor has the added value of control over the efficiency of the intramolecular energy transfer process by switching between the trans and cis isomer. Thus, the presented dendrimer not only serves as a model system for studies of photoswitching of intramolecular energy transfer processes but may also have potential applications, for instance, as a photoswitched light-harvesting system.

The target dendritic host **1** (as shown in Figure 2) that has been synthesized here fulfills the following requirements:

(i) a rigid scaffold based on a third-generation PPD,
(ii) an AB in the middle of each dendron (every AB acts as a "hinge" and the combination of eight "hinges" may generate photoswitchable voids),
(iii) basic pyridyl functions in the interior for enhancing host−guest (H−G) interactions,
(iv) a fluorescent chromophore to enable fluorescence tracking in potential cell experiments (for our ultimate purpose being an aqueous drug delivery system), and
(v) an energy donor−acceptor system consisting of AB as donor and PDI as acceptor allowing control of intramolecular energy transfer processes by photoswitching of AB.

The steric congestion between phenoxy groups in all four PDI bay positions enforces a slight twisting of the PDI plane and, more importantly, an orthogonal orientation of all substituents (and thus dendrons) with regard to that plane. Model structures suggest that the rigid dendrons spatially extend into opposing directions in the all-trans isomer ("open" structure), while pointing toward each other in the all-cis isomer ("closed" structure). As a consequence, voids in the dendritic interior are easily accessible for potential guest molecules in the "open" form, while they are sterically shielded with rigid and bulky polyphenylene dendrons in the "closed" form. Moreover, the model structures suggest that a third-generation dendrimer is ideal: lower generations result in insufficient shielding of voids, while in higher generations steric hindrance obstructs isomerization.

2. RESULTS AND DISCUSSION

2.1. Synthesis. The targeted dendritic host **1** was synthesized in 15 steps. The key building block for its synthesis is the AB-, ethynyl- and pyridyl-functionalized tetracyclone **12**. It was prepared in seven steps starting from *p*-bromoaniline **2** (Scheme 1).

Sonogashira coupling of (triisopropylsilyl)acetylene with *p*-bromoaniline (**2**) afforded ethynyl-functionalized aniline **4**, and oxidation of *p*-bromoaniline (**2**) with ozone[65] afforded nitrosobenzene **3** in almost quantitative yield. Azo-coupling of both products **3** and **4** yielded the asymmetrically substituted azobenzene **5**. The selected sequential order of coupling reactions (route 1) avoids the necessity of performing the Sonogashira coupling selectively (in route 2).

Boron-ester funtionalized benzil **8** was synthesized from 4,4′-dibromobenzil **7** using an excess amount of bis(pinacolato)-diboron in the presence of $Pd(dppf)Cl_2$ and potassium carbonate. Suzuki coupling of benzil **8** and asymmetrically substituted AB **5** then furnished the AB- and ethynyl-functionalized key intermediate **9**. It is noteworthy, however, that thorough purification of benzil **8** [removal of trace amounts of bis(pinacolato)-diboron] prior to Suzuki coupling is crucial to avoid homocoupling of **5**. The 1,3-dipyridin-2-ylpropan-2-one **11** was obtained by nucleophilic addition of picolyllithium (generated from phenyllithium and 2-picoline) to 2-pyridylacetonitrile followed by acidic hydrolysis of the imine intermediate.[66]

Finally, the Knoevenagel condensation between AB- and ethynyl-functionalized benzil **9** and pyridyl-functionalized propanone **11** provided the key building block **12**. Surprisingly, an alternative reaction sequence via Knoevenagel condensation of dibromobenzil **7** and dipyridinylacetone **11** was not successful. Possibly, the solubility of dibromobenzil **7** in *tert*-butanol is too low even at high temperatures.

Ethynyl functionalization of the PDI core was achieved in three steps starting from tetrachloro-PDI **13** following the literature procedure.[50] Diels−Alder cycloaddition of key building block **12** to the so functionalized PDI core **14** afforded the first-generation dendrimer **15** (Scheme 2). Successive deprotection and cycloaddition with tetracyclone or $Cp(TIPS)_2$ building blocks[42,43] gave the dendrimer G_2-end-capped **17**, G_2-$(TIPS)_{16}$ **18**, and finally the target dendrimer **1**.

All compounds were characterized by ^1H and ^{13}C NMR spectroscopy, MALDI-TOF mass spectrometry, UV−vis absorption spectroscopy, FTIR spectroscopy, melting point, and elemental analysis. The dendrimers **1** and **15**−**19** were also characterized by fluorescence emission spectroscopy (analytical data are available in the Supporting Information).

2.2. The Photochemical Cis−Trans Isomerization. With the successful synthesis of dendrimer **1**, eight AB moieties

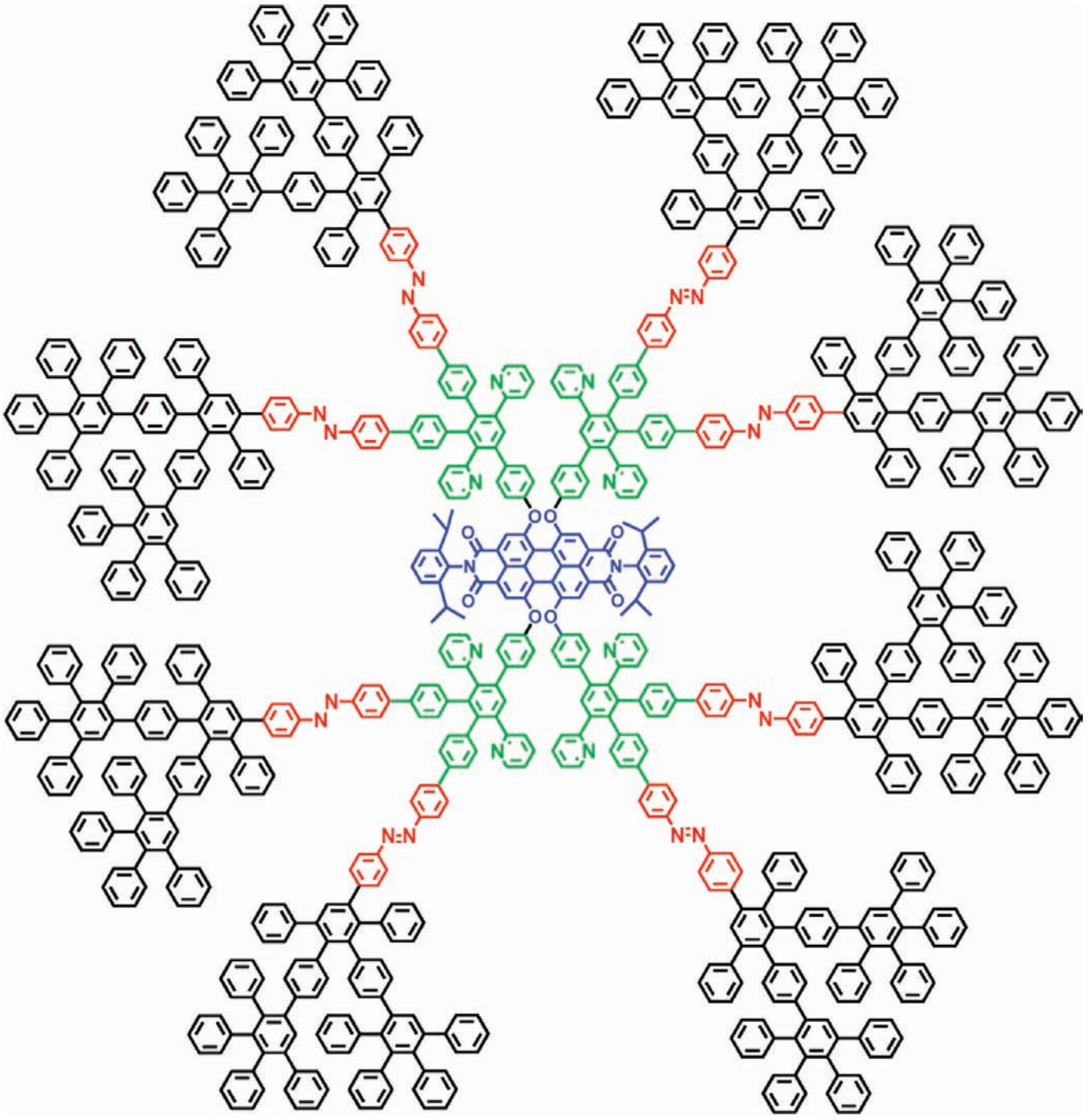

Figure 2. Chemical structure of the dendritic host **1**.

have been placed into a rigid dendritic scaffold. The UV−vis absorption spectrum of dendrimer **1** has three characteristic absorption bands with maxima at 254 nm (absorption of phenyl rings), 500−600 nm (absorption of the PDI core) and, most importantly, at 370 nm ($\pi-\pi^*$ transition of *trans*-AB).[67] The intensity of the absorption band at 370 nm correlates to the amount of *trans*-AB isomer in the solution (Figure 4).

A 2.5×10^{-6} M solution of dendrimer **1** in methylene chloride was exposed to UV light of 365 nm in order to induce the isomerization of AB from trans to cis. Figure 4 shows the absorption spectra before (solid black curve) and after 12 min of irradiation (solid blue curve).

Compared to the nonirradiated solution, the absorption band at 370 nm clearly decreases, while the absorption band at 460 nm ($n-\pi^*$ transitions of *cis*-AB)[67] increases slightly. The change of absorption band intensities induced by UV irradiation indicates a conversion of the all-trans dendrimer **1**(8t) into species containing on average three trans and five cis AB moieties, namely, **1**(3t5c), in the photostationary state (PSS) (see Figure 1 of the Supporting Information). The quantum yield of the **1**(8t)→**1**(3t5c) photoisomerization reaction was determined to

Scheme 1. Synthesis of Key Building Block Tetracyclone 12[a]

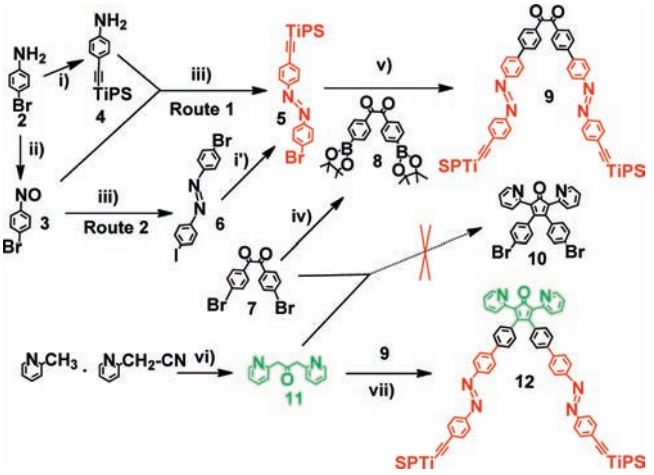

[a] Reaction conditions: (i) $Pd(PPh_3)Cl_2$, (triisopropylsilyl)acetylene, toluene/TEA, 80 °C, 12 h, 60%; (i′) similar to condition i but at 0 °C to rt, 90%; (ii) $2KHSO_5 \cdot KHSO_4 \cdot K_2SO_4$, DCM/$H_2O$, 4 h, 92%; (iii) AcOEt/AcOH, 50 °C, 12 h; 86%, (iv) bis(pinacolato)diboron, Pd-(dppf)Cl_2, AcOK, dioxane, 80 °C, 24 h, argon, 90%; (v) $Pd(PPh_3)$, CuI, PPh_3, nBu_4NBr, toluene/H_2O, 80 °C, argon, 93%; (vi) (a) phenyllithium, reflux (b) H_3O^+, 70%; (vii) tBuOH, nBu_4NOH, 80 °C, 2 h, 65%.

Scheme 2. Synthesis of 1 [a]

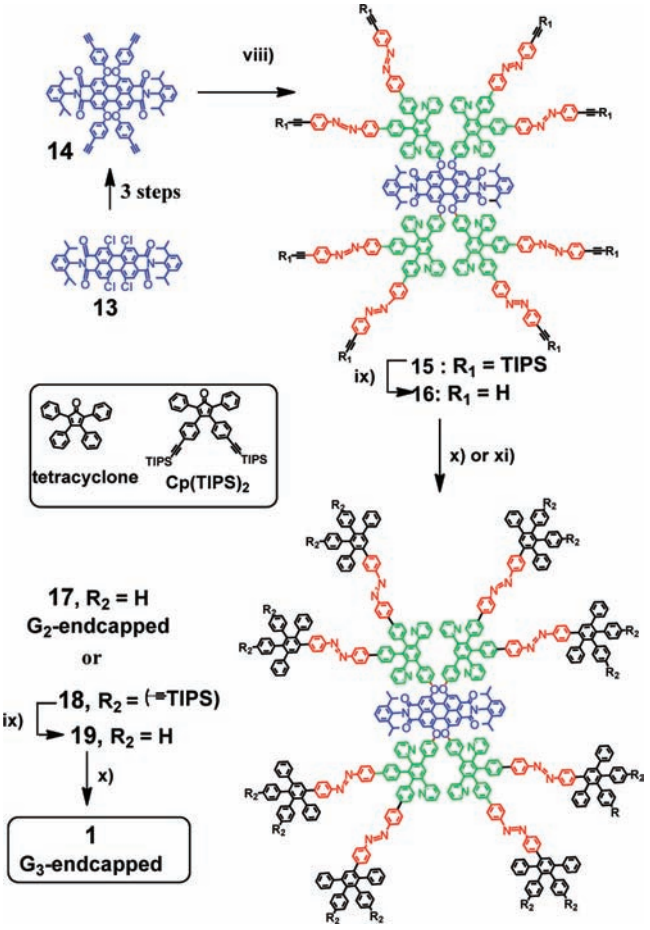

[a] Reaction conditions: (viii) *o*-xylene, **12**, 145 °C, 24 h, 90%; (ix) nBu_4NF, THF, rt, 3 h [affords **16** (87%) or **19** (92%)]; (x) *o*-xylene, tetracyclone, 145 °C, 48 h [affords **17** (98%) or **1** (92%)]; (xi) *o*-xylene, $Cp(TIPS)_2$, 145 °C, 48 h [affords **18** (91%)].

be $\Phi_{t\text{-}c} = 0.114$ (inset of Figure 4 and Supporting Information Figure 2). Due to the nonlinear characteristic of the apparent quantum yield values versus times, the maximum quantum yield was determined by extrapolating the linear region to zero time, corresponding to the first four Φ values within the first 2 min of the photoisomerization reaction.

The solution of **1**(3t5c) was then irradiated with visible light of 450 nm to induce the back isomerization from cis to trans. Consequently, the absorption band at 370 nm recovers its initial intensity,[68] indicating the back conversion of **1**(3t5c)→**1**(8t) with quantum yield $\Phi_{c\text{-}t} = 0.794$ (see Supporting Information Figure 3). Thus, UV−vis measurements thus demonstrate that AB moieties can undergo reversible photoisomerization within the rigid scaffold of dendrimer **1**. Furthermore, Figure 4 shows that the photoisomerization proceeds while maintaining isosbestic points up to the PSS, which demonstrates the photostability of AB moieties and the dendrimer upon irradiation with UV light.

By plotting the change of absorbance versus time (Supporting Information Figure 8), the rate constant of cis-to-trans (k_{ct}) photoisomerization of AB moieties in **1** was determined to be $1.80 \pm 0.18\ min^{-1}$. In contrast to the light-driven isomerization, the thermally driven cis-to-trans isomerization of AB moieties within **1** (Figure 5) occurs much more slowly [$k_{ct,thermal} = (8.15 \pm 0.40) \times 10^{-4}\ min^{-1}$, only about 4.5×10^{-4} times the rate constant of the light-driven process]. The small value of $k_{ct,thermal}$ indicates that the cis conformation in **1** is maintained for a reasonably long time ($t_{1/2} = 14.2$ h) despite relatively high steric repulsion between dendrons.

In order to examine the effect of dendron size (potential steric obstruction) on the photoisomerization of AB, the rate constants of trans-to-cis isomerization were also measured as a function of dendrimer generation (from G_1 to G_3 at the same concentration). Surprisingly, the rate constants of all dendrimers were found to be on the same order of magnitude, which indicates that an increasing dendron size does not substantially impede AB isomerization. Such modest variance in rate constants with dendrimer size has also been reported for rigid dendrimers using AB as the core.[19]

Dendrimer **1** exhibits good photostability, as was confirmed by excellent recovery of the respective isomers upon alternately exposing a solution of **1** to light of 365 and 450 nm wavelength (Figure 6).[69]

In a sequence of 20 "switchings" between cis and trans, we found no indication of efficiency decrease or degradation.

The structural model of **1** (Figure 3) indicates that photoisomerization should induce a drastic change in molecular size and volume. To investigate the effect of photoisomerization on the molecular size of **1**, its hydrodynamic volume was determined by means of size exclusion chromatography (SEC) before **1**(8t) and after **1**(3t5c) irradiation at 365 nm.

After irradiation at 365 nm, **1** showed a significant increase in elution volume (Figure 7), indicating a marked decrease of its hydrodynamic volume of about 40%.[70]

To further support our findings, the changes in hydrodynamic volume were also determined by spectroscopic methods. While the presence of the fluorescent PDI chromophore in dendrimer **1** precluded determination of the hydrodynamic radius r_H via dynamic light scattering (DLS), it enabled the study of **1** via fluorescence correlation spectroscopy (FCS). The latter allows

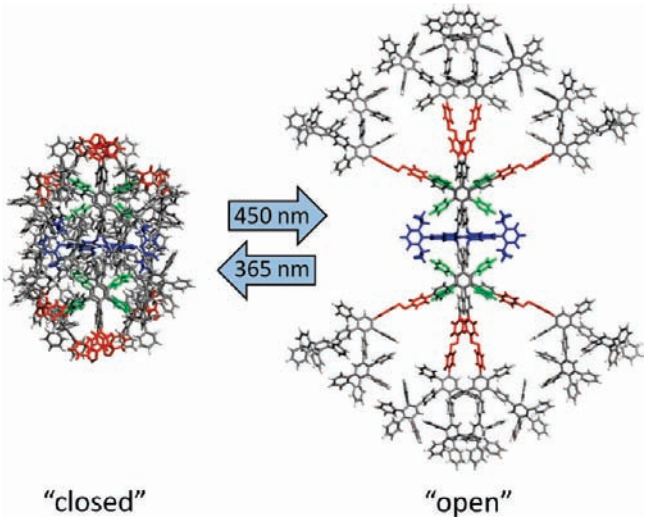

Figure 3. Model structures of the dendritic host system in all-cis and all-trans conformation.

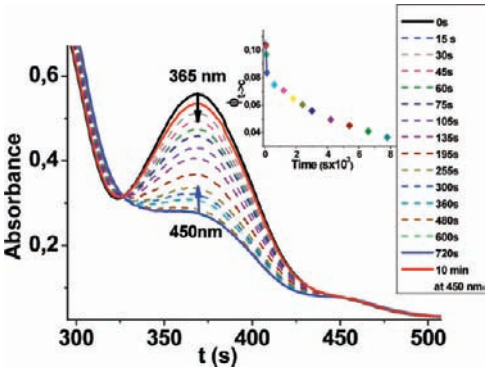

Figure 4. Reversible change in the absorption band of **1** at 370 nm as a function of irradiation time at 365 and 450 nm (2.5×10^{-6} M solution of **1** in CH_2Cl_2 at 298 K): solid black line, no irradiation; solid blue line, PSS reached after 720 s of exposure to 365 nm light; dashed curves, absorption changes with time upon being exposed to 365 nm UV light; solid red line, PSS solution after 300 s of exposure to 450 nm light;[68] inset, apparent quantum yield values as a function of time, where the extrapolation of quantum yield values of the first two minutes to zero time is used for determining the real quantum yield of the trans → cis process of **1** (for the quantum yield of the cis-to-trans process see the Supporting Information).

determination of the diffusion properties of fluorescent tracers with extremely high sensitivity down to the single molecule level, and with higher precision compared to DLS.

A highly diluted solution (10^{-7} M) of **1** in CH_2Cl_2 was excited by a 543 nm laser. This wavelength matches the absorbance of the PDI core and does not influence the photoisomerization of AB.

FCS measurements (Figure 8) clearly show a decrease in diffusion time of dendrimer **1** after irradiation at 365 nm (trans→cis), which corresponds to a drastic decrease of the hydrodynamic radius from 3.59 ± 0.19 nm before irradiation to 2.49 ± 0.09 nm after irradiation. These radii correspond to volumes of 194 and 65 nm^3, respectively, and thus a volume decrease of about 66%.[71] Such pronounced decrease in volume upon cis−trans isomerization has not yet been reported. This result proves that the rigidity of the dendritic scaffold and the specific positioning of ABs

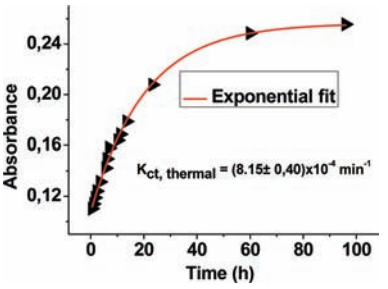

Figure 5. Determination of the rate constant of thermal cis-to-trans isomerization for a 1.5×10^{-6} M solution of **1**(3t5c) in CH_2Cl_2 obtained after being irradiated at 365 nm for 10 min. The change of absorption intensity at 370 nm was plotted against time and fitted exponentially to derive the rate constant.

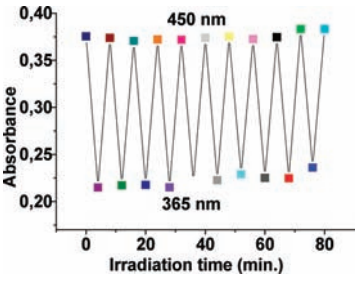

Figure 6. Change in absorption of **1** at 370 nm upon 10 irradiation cycles (alternating irradiation at 365 and 450 nm).[70]

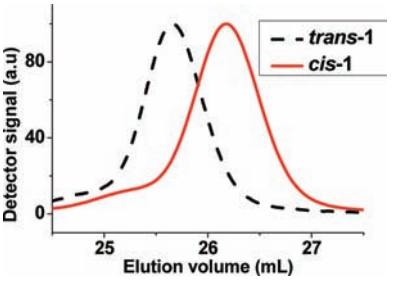

Figure 7. SEC traces of solutions of **1** before and after 10 min of exposure to 365 nm light. Conditions: THF, 1 mL/min, 500 Å, 10^4 Å, 10^6 Å SDV (Polymer Standard Service Mainz) columns (0.8 × 30 cm), ambient temperature.

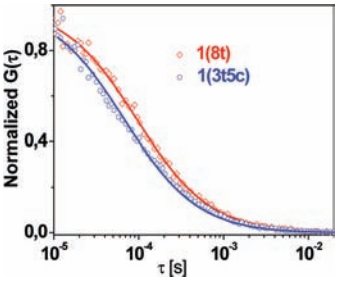

Figure 8. FCS results: normalized autocorrelation functions of **1** before (blue) and after 10 min of exposure to 365 nm light (red) (solution 10^{-7} M of **1** CH_2Cl_2).

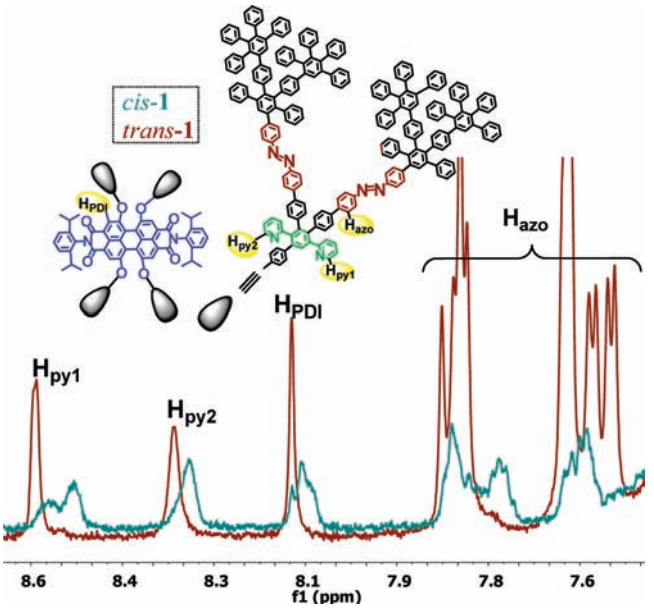

Figure 9. (Top) Molecular structure of **1** with some peak assignmen. (Bottom) Partial ^{1}H NMR spectrum of **1**(8t) (red) and **1**(3t5c) (blue) (700 MHz, CD_2Cl_2, 295 K).

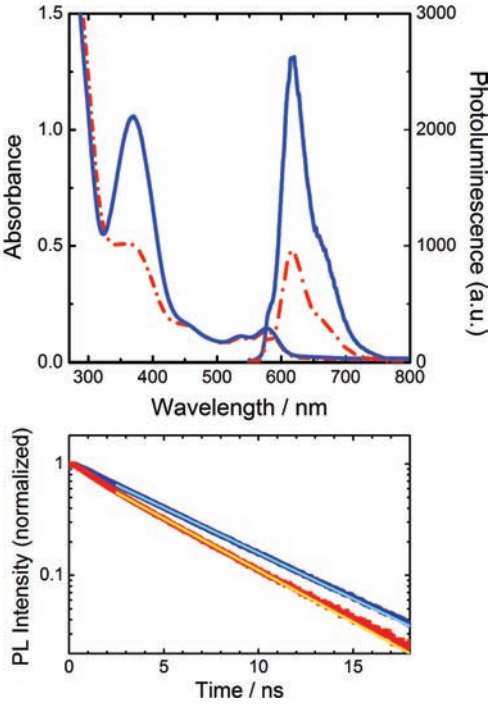

Figure 10. The upper panel shows the absorption and fluorescence spectra of **1**(8t) (blue) and **1**(3t5c) (red). The emission spectra were recorded after excitation at 570 nm. The lower panel shows the PL decay transients (dots) for **1**(3t5c). and **1**(8t) and single exponential fits (solid lines).

therein are crucial for a drastic change of dendrimer size upon photoswitching.

The model structures (Figure 3) indicate that dendrimer **1** becomes much more compact upon switching from the trans to the cis isomer. In the cis isomer, protons of both the core and dendrons should be noticeably shielded by densely packed polyphenylenes in their close environment as compared to the trans isomer. To detect such changes in the chemical environment of specific protons, ^{1}H NMR spectra of dendrimer **1** were recorded before and after irradiation at 365 nm (Figure 9 and Supporting Information Figure 4).[72]

The ^{1}H NMR spectrum of dendrimer **1** after irradiation [**1**(3t5c), blue] shows two major differences as compared to the spectrum before irradiation [**1**(8t), red].

First, in **1**(3t5c), many proton signals (H_{py}, H_{PDI}, H_{azo}, $H_{periphery}$) experience a slight upfield shift, probably due to better local screening from the overall magnetic field by surrounding polyphenylenes. Indeed, it was indicated previously that some azo groups remain in the trans form; thus, there should be some signals due to the trans form, and this trans form should create a different environment for some cis azo groups. Also, specific protons give rise to more than one defined signal in **1**(3t5c) as compared to **1**(8t), which may be due to the simultaneous existence of slightly different environments for such protons in different **1**(3t5c) conformers. ^{1}H NMR spectra thus clearly reflect the increased density of polyphenylenes surrounding the dendritic core after irradiation at 365 nm. The switchability of polyphenylene density around the dendritic core is an important prerequisite to enable active encapsulation of guest molecules into internal cavities of **1**.

2.3. Photoswitchable Intramolecular Energy Transfer. The PDI core of **1** can be used as a sensitive fluorescent probe. Here, we demonstrate that the photoisomerization of the AB groups switches significantly the efficiency of intramolecular energy transfer from AB to PDI. Although photoswitching of intramolecular energy transfer has previously been reported for dyads,[73−75] this is, to the best of our knowledge, the first example of photoswitching of intramolecular energy transfer within a dendritic structure from AB to PDI. Previous work, for instance by Feng and co-workers[76] on linear perylenediimide−azobenzene dyads, has demonstrated a conformation-related change of the fluorescence efficiency due to PDI excimer formation, if PDI molecules come close enough in one of the isomers.

Table 1. Photoluminescence Quantum Efficiencies (PLQE) of 1(8t) and *cis*-1 Excited at 550 nm (i.e., PDI absorption) and 365 nm (i.e., absorption of the azo group)

	550 nm	365 nm
1(8t)	≈1	0.30 ± 0.10
1(3t5c)	0.34 ± 0.10	0.37 ± 0.10

Figure 10 shows a comparison of the absorption and fluorescence spectra of **1**(8t) and **1**(3t5c). The absorption maximum of **1**(3t5c) at 370 nm is about half of that of **1**(8t) at 370 nm. The fluorescence spectra obtained upon direct excitation of the PDI core at 570 nm are virtually the same for **1**(3t5c) and **1**(8t). However, the emission intensity of **1**(3t5c) is much lower than that observed for **1**(8t), despite similar absorption at 570 nm. We determined the photoluminescence quantum efficiency (PLQE) of **1**(8t) and **1**(3t5c) in solution, as shown in Table 1.

The PLQE of **1**(8t) upon excitation of the PDI core at 550 nm is unity within the experimental error, whereas a substantially lower quantum efficiency of 34% is found for **1**(3t5c). Thus, it appears that the steric crowding in **1** (3t5c) decreases the PLQE of the PDI core. The fluorescence transients of **1**(8t) and **1**(3t5c) (shown in the bottom panel of Figure 10) fit well to single

Table 2. Parameter of the Single Exponential Fits [according to $y = A_1 \exp(-x/t_1)$] to the Decay Transients Shown in the Lower Panel of Figure 10

	A_1	t_1/ns
1(8t)	1.0336 ± 0.0005	5.327 ± 0.002
1(3t5c)	0.9433 ± 0.0012	4.674 ± 0.005

exponential decays, as shown in Table 2, showing a slightly shorter fluorescence lifetime of the PDI chromophore in **1** (3t5c).

However, the observed lifetime difference cannot account for the decrease of the PLQE of **1**(3t5c). In fact, the fluorescence quenching must occur in the first 1 ns after excitation, i.e., much faster than the time resolution of our experiment, indicating that a rapid deactivation process quenches a considerable fraction of the PDI excited states. Upon excitation at 365 nm the PLQE of **1**(8t) is only one-third that of the PLQE at 550 nm excitation, indicating that the intramolecular energy transfer from the azobenzene groups to the PDI core is incomplete. This appears reasonable because some of the absorbed photons drive the trans to cis photoisomerization reaction and thus will not create excited states that can be transferred to the PDI core; however, there must be an additional deactivation process for the excited states of the AB units to explain the moderate quantum efficiencies, as we will show below by ultrafast transient absorption spectroscopy.

Applying the same conditions to **1**(3t5c) shows a PLQE of about 37%, similar to the PLQE observed upon direct excitation of the PDI chromophore of **1**(3t5c). We exclude direct excitation of the PDI at 365 nm, since the absorbance of the PDI is negligible at this wavelength in comparison to the absorbance of the AB units. Thus, within the experimental error of our PLQE measurement, the efficiencies of **1** (3t5c) are similar, irrespective of direct excitation of the PDI core or excitation of the AB units and subsequent energy transfer to the PDI core. This in turn implies that in **1**(3t5c) the energy transfer from the azobenzene units to the PDI core is very efficient. The higher fluorescence efficiency of **1**(3t5c) upon excitation at 365 nm can also be observed by a direct comparison of intensity-calibrated fluorescence spectra, which show stronger emission from **1**(3t5c) than **1**(8t) (Supporting Information Figure 5), unlike that seen for direct excitation of the PDI core at 570 nm. Hence, our results show that we could successfully gain control over the efficiency of intramolecular energy transfer from AB to PDI in **1** by simple photoswitching of AB. This opens up several possibilities to design novel donor−acceptor-type dendrimers with photoswitchable energy transfer properties having potential applications, for instance, as photon-harvesting molecules for photon energy conversion.

In order to get a better insight into the excited state dynamics of **1**(8t) upon excitation at 365 and 550 nm, we performed ultrafast transient absorption (TA) experiments on the dendrimer in solution. The upper panel of Figure 11 shows the TA spectra of the trans-isomer at increasing delay times after excitation of the PDI core at 570 nm.

The spectra exhibit the TA features typically seen for PDI chromophores. Between 550 and 650 nm a combination of ground state bleaching and stimulated emission can be found. An isosbestic point at 650 nm points to the presence of a single excited species, i.e., singlet excited states of the PDI chromophore. At wavelength longer than 650 nm the typical photoinduced

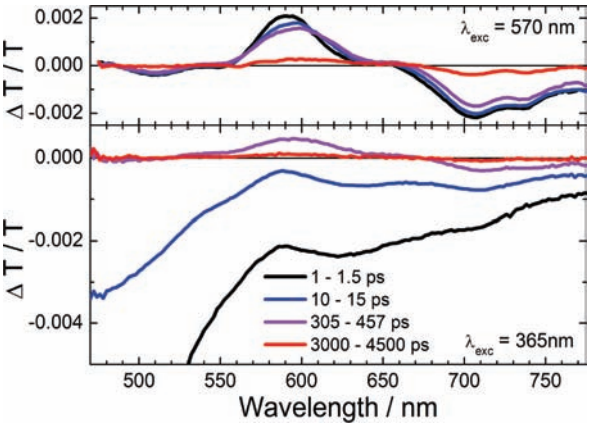

Figure 11. Transient absorption spectra of **1**(8t) excited at 570 nm (upper panel) and 365 nm (lower panel). After excitation of the azobenzene (at 365 nm), an intense and broad photoinduced absorption (PA) of the azobenzene group covers all other signals. However, the induced absorption decays much faster than the excited states of the PDI and thus the PDI bleach and PA become visible after about 100 ps.

absorption (PA) of excited singlet states of PDI chromophores can be observed. In comparison to the spectra obtained after excitation at 570 nm, the bottom panel of Figure 11 shows the TA spectra of **1**(8t) at different delay times after excitation at 365 nm. Here, a broad and intense photoinduced absorption of the azobenzene groups clearly dominates the spectra at early times. However, after about 100 ps the broad PA signal of the azobenzene groups has vanished and the typical TA features of the PDI chromophore can be observed in the TA spectra (compare also upper panel of Figure 11). A singular value decomposition (SVD) analysis of the TA data set indicated the presence of two main processes that dominate the photophysics. First, some excitons on the AB units undergo a rapid energy transfer to the PDI core, leaving a fraction of the previous excitations on the PDI, which subsequently decay with the same lifetime of several nanoseconds observed for the excitation at 570 nm. The presence of an energy transfer process is also supported by the PL and PLQE measurements shown above that demonstrate emission from the PDI chromophore upon excitation of the dendrimer at 365 nm, although the absorbance of the PDI chromophores with respect to the AB units is negligible at this wavelength. Second, a rapid deactivation process of a fraction of the excited states of the azobenzene moieties within a few tens of picoseconds occurs. The latter is also supported by the dynamics of the TA signal in the region of the PDI photoinduced absorption, which shows a rapid initial drop of the signal due to fast deactivation of the excited states on the azobenzene groups (see Supporting Information Figure 7). Hence, it is not possible to entirely disentangle the energy transfer process from the AB units to the PDI core, since the intrinsic decay occurs on a similar time scale and the features of the PDI chromophores are entirely superimposed by the comparably strong PA of the AB units, which complicates the data analysis. However, the TA experiments clearly demonstrate that the energy transfer to the PDI and intrinsic decay of the excited states on the AB units occur within a few tens of picoseconds, which is rapid enough to create a considerable amount of excited states on the PDI core and explains the substantial quantum efficiency of the PDI even for the all-trans dendrimer after excitation at 365 nm.

2.4. Guest Uptake and Photoswitchable Encapsulation and Release. Prior to a study on active guest encapsulation, the general ability of dendrimer **1** to act as a host for guest molecules was investigated. Host−guest studies are often performed by using fluorescent guest molecules and detecting changes in their fluorescence output signal as an indicator for changes in their chemical environment. However, the dendritic host **1** already contains two different types of chromophores (PDI and AB), rendering a study by fluorescence detection inadequate. Instead, a simple, nonfluorescent molecule, *p*-nitrophenol (*p*-NP), was chosen as the guest for uptake studies by means of NMR and UV−vis spectroscopy.

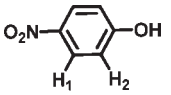

p-nitrophenol

p-Nitrophenol fulfills some important requirements regarding both guest uptake and later encapsulation studies:

(i) *p*-NP exhibits ^{1}H NMR signals with distinct chemical shifts compared to host **1** (facile detection of potential signal changes in the NMR spectra of host−guest mixtures).

(ii) *p*-NP bears one phenolic proton (potential formation of hydrogen bonds to pyridin moieties of the host).

(iii) *p*-NP is soluble in methanol, while the host **1** is insoluble and precipitates. This solubility difference enables a facile separation of host and guest.

The guest uptake experiment was performed directly in a NMR tube containing a 10^{-3} M solution of **1** in CD_2Cl_2. Upon adding 2 equiv of *p*-NP, the signal ascribed for the phenolic proton of *p*-NP disappeared and the signal of H_1 significantly shifted upfield (see Supporting Information Figure 6).

Similarly, signals assigned to protons of the interior cavities of **1** (H_{azo}, H_{G1}, and H_{PDI}) shifted upfield while other proton signals of **1** (e.g., peripheral protons) did not, indicating that the majority of guests molecules resides in the dendrimer cavities (see Supporting Information Figure 4). Surprisingly, the phenolic proton of *p*-NP did not show significant hydrogen bonding to the pyridyl functions of the host, despite its relatively high acidity. Only a large amount of guest (more than 10 equiv) induced a slight upfield shift of H_{py} along with the emergence of two new H_{py} peaks (Figure 12). Probably, the N atoms in the ortho-positions exhibit only a limited accessibility toward guests. In order to better enhance guest uptake by hydrogen bonds, the N atom could in the future be placed in the meta- or para-position. However, despite of negligible H-bond interaction between host **1** and guest *p*-NP, the guest was still preferably directed toward interior cavities of the host.

Host−guest interactions were also investigated by UV−vis spectroscopy. Figure 13 shows the absorption spectrum of the free guest *p*-NP and of the guest in the presence of host **1** (guest/host = 10/1). Due to the overlapping absorption spectra of host and guest species, the spectrum of the guest in the presence of host **1** was obtained by subtraction of the spectrum of **1** from that of the mixture.

As demonstrated in Figure 13, the guest absorption band exhibits a hypsochromic shift in the presence of only 0.1 equiv of host **1** as compared to the absorption band in the absence of host. The shift indicates a change in the chemical environment of the guest. The change is probably caused by the transition of guest molecules from the more polar solution to the less polar environment of dendritic cavities.

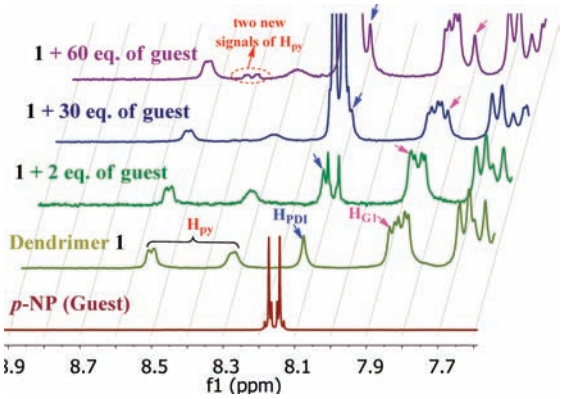

Figure 12. Details of ^{1}H NMR spectra (300 MHz, CD_2Cl_2, 295 K) of titration experiment upon increasing the number of guests.[77]

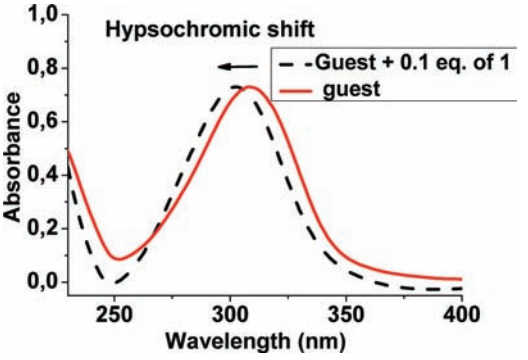

Figure 13. Absorption spectra of *p*-nitrophenol in CH_2Cl_2 at 298 K: red curve, in absence of host **1**; dashed black curve, in the presence of host **1**.

After demonstrating the ability of host **1** to take up *p*-NP guests, we wondered whether it would be possible to permanently encapsulate such guests into internal cavities of **1** by switching from the "open" to the "closed" form. Therefore, a solution mixture (3 mL) of the dendritic host **1** (0.25M, 1 equiv) and guest molecules *p*-NP (5M, 20 equiv) was irradiated at 365 nm to induce the "closing" of **1** by trans-to-cis isomerization of its AB moieties (Figure 14A,B). By doing so, the fraction of guest molecules that resided in the interior cavities of **1** before switching should now be encapsulated therein. This experiment was repeated three times. A control experiment was performed in parallel, in which the solution was not irradiated at 365 nm and thus no encapsulation of guest molecules should have occurred.

Both solutions were concentrated by evaporation of three-quarters of their solvent. The concentrated solutions were then added dropwise into methanol. Due to the different solubility of host and guest in methanol, the host **1** precipitated completely, while guest molecules remained completely dissolved. After separation of the host **1** from the solution by centrifuge and filtration, the precipitate was thoroughly washed twice with fresh methanol in order to remove remaining guest molecules that might have been superficially adsorbed (Figure 14C,C′). After drying, the precipitated host **1** was dissolved in deuterated methylene chloride and measured by ^{1}H NMR spectroscopy (Figure 14,D,D′).

dx.doi.org/10.1021/ja2022398 |*J. Am. Chem. Soc.* 2011, 133, 11194–11204

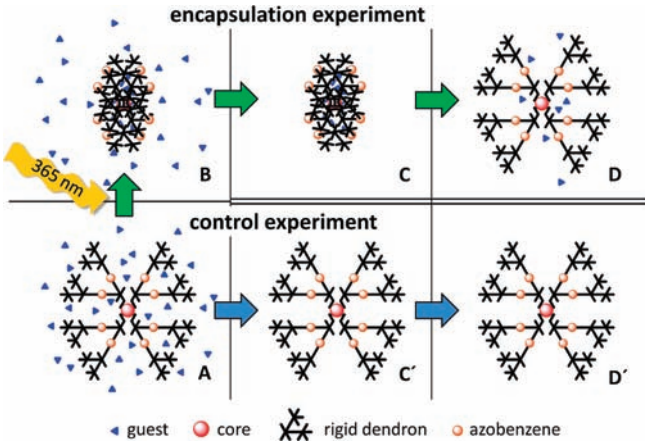

Figure 14. Encapsulation experiment (green arrows) and control experiment (blue arrows): (A) solution of host and guest in methylene chloride, (B) photoinduced "closing" of the host, (C) separation and washing of host with methanol, (D) detection of potential guests via ^{1}H NMR.

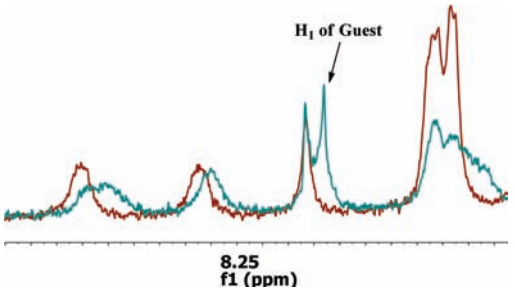

Figure 15. ^{1}H NMR spectrum of the complex host−guest in the encapsulation experiment (blue line) and in the control experiment (red line). Two guests per host **1** were observed only in the encapsulation experiment.

As expected, not even trace amounts of guest molecules could be detected in any control experiment, where the dendritic host **1** remained in the "open" conformation all the time.

By contrast, an average of about 2 equiv[78] of guest molecules per dendrimer was detected in the experiments where the dendritic host **1** had previously been switched to the "closed" conformation (Figure 15). The guest molecules could be released either by irradiation of the "closed" host with blue light or by the slow thermal process of cis-to-trans isomerization. These results clearly demonstrate that guest molecules can indeed be entrapped into suitably designed hosts via a photoswitched mechanism, as proposed in the Introduction.

3. CONCLUSION

We have demonstrated the successful synthesis of a fluorescent dendritic host with photoswitchable properties. Our design utilizes the unique rigidity of the PPD scaffold for a site-specific placement of three different types of function (PDI, pyridine, and azobenzene).

The employment of eight azobenzene moieties as hinges in defined positions of the rigid scaffold enables the photoswitchability of (i) molecular size, (ii) intramolecular energy transfer, and (iii) guest encapsulation and release. The magnitude of change in molecular size upon photoisomerization (66% decrease in hydrodynamic volume upon trans-to-cis isomerization, as confirmed by FCS) is unprecedented as compared to earlier AB-functionalized dendrimers.[22]

The fluorescent PDI core allows for a tracking of the dendritic host by fluorescence techniques, such as confocal microscopy or stimulated emission depletion (STED) microscopy. Additionally, it can be used as a sensitive optical probe of intramolecular energy transfer processes. In fact, we could not only show intramolecular energy transfer within the dendrimer, as already reported for other donor−acceptor-type dendrimers, but we could also demonstrate that the efficiency of the intramolecular energy transfer is greatly enhanced in **1**(3t5c) compared to **1**(8t). Thus, dendrimer **1** is to the best of our knowledge the first example for efficient photoswitching of intramolecular energy transfer in a dendritic structure using AB as donor and PDI as acceptor.

The presence of *o*-pyridyl functions only had a minor contribution to the direction of guest molecules into dendritic cavities. Nevertheless, sufficient uptake of *p*-NP guests was confirmed by NMR and UV−vis spectroscopy.

Finally, we have demonstrated that the photoswitchability of the host can be utilized actively to encapsulate guest molecules into its interior cavities. This novel, light-driven encapsulation mechanism has important implications for the design of new drug delivery systems. It could prevent premature leaching of drugs from their hosts without the requirement of covalent linking and thus enable the delivery of unmodified and active drugs. The number of encapsulated guests might be further increased in the future by way of fine adjustments of the host design, including the size of its interior cavities and their functionalization. Host−guest interactions could be further enhanced by incorporating different groups (such as *p*-pyridyl or pyridinone) in the place of *o*-pyridyl functions. Since applications in a biologic environment require both water solubility and biocompatibility, our current work is focused on changing the solubility and membrane permeability properties of our dendritic host via suitable functionalization of its periphery.

■ ASSOCIATED CONTENT

Supporting Information. Experimental details including procedures for preparation and full characterization of compounds **1**, **3**, **4**−**6**, **8**, **9**, **12**, and **15**−**19** and figures as noted in the text. This material is available free of charge via the Internet at http://pubs.acs.org.

■ AUTHOR INFORMATION

Corresponding Author
muellen@mpip-mainz.mpg.de

■ ACKNOWLEDGMENT

We thank Prof. Dr. Martin Baumgarten, Khalid Chiad, Oliver Dumele, and Qui Su for their support; Chen Li for his fruitful discussions, Dr. Kaloian Koynov for FCS measurement, Sandra Seywald for GPC measurements; Manfred Wagner and Petra Kindervater for NMR measurements; and Stephan Türk for MALDI-TOF measurements.

REFERENCES

(1) Zaporojtchenko, V.; Strunskus, T.; Zargarani, D.; Herges, R.; Faupel, F. *Nanotechnology* **2010**, *21*, 465201.
(2) Li, Y.; Jia, X.; Gao, M.; He, H.; Kuang, G.; Wei, Y. *J. Polym. Sci. Polym. Chem.* **2010**, *48*, 551.
(3) Tomasulo, M.; Deniz, E.; Benelli, T.; Sortino, S.; Raymo, F. M. *Adv. Funct. Mater.* **2009**, *19*, 3956.
(4) Klajn, R.; Wesson, P. J.; Bishop, K. J. M.; Grzybowski, B. A. *Angew. Chem., Int. Ed.* **2009**, *48*, 7035.
(5) Sugiura, S.; Sumaru, K.; Ohi, K.; Hiroki, K.; Takagi, T.; Kanamori, T. *Sensor Actuators A-Phys.* **2007**, *140*, 176.
(6) Kimura, K. ; Sakamoto, H.; Nakamura, T. *J. NanoSci. Nanotechnol.* **2006**, *6*, 1741.
(7) Yu, Y.; Nakano, M.; Ikeda, T. *Nature* **2003**, *425*, 145.
(8) Yasuda, S.; Nakamura, T.; Matsumoto, M.; Shigekawa, H. *J. Am. Chem. Soc.* **2003**, *125*, 16430.
(9) Shimoboji, T.; Larenas, E.; Fowler, T.; Kulkarni, S.; Hoffman, A. S.; Stayton, P. S. *Proc. Natl. Acad. Sci. U. S. A.* **2002**, *99*, 16592.
(10) Ichimura, K.; Oh, S.-K.; Nakagawa, M. *Science* **2000**, *288*, 1624.
(11) Khan, I. M.; Harrison, J. S. (Eds.) *Field Responsive Polymers. Electroresponsive, Photoresponsive, and Responsive Polymers in Chemistry and Biology*; Oxford University Press: Oxford, U.K., 1999.
(12) Moore, J. S. *Acc. Chem. Res.* **1997**, *30*, 402.
(13) Trie, M. *Pure Appl. Chem.* **1990**, *62*, 1495.
(14) Burakowska, E.; Zimmerman, S. C.; Haag, R. *Small* **2009**, *5*, 2199.
(15) Hartley, G. S. *Nature* **1937**, *140*, 281.
(16) Deloncle, R.; Caminade, A.-M. *J. PhotoChem. Photobiol. C. Photochem. Rev.* **2010**, *11*, 25.
(17) Puntoriero, F.; Bergamini, G.; Ceroni, P.; Balzani, V.; Vagtle, F. *New J. Chem.* **2008**, *32*, 401.
(18) Puntoriero, F.; Ceroni, P.; Balzani, V.; Bergamini, G.; Vögtle, F. *J. Am. Chem. Soc.* **2007**, *129*, 10714.
(19) Liao, L.-X.; Stellacci, F.; McGrath, D. V. *J. Am. Chem. Soc.* **2004**, *126*, 2181.
(20) Weener, J. W.; Meijer, E. W. *Adv. Mater.* **2000**, *12*, 741.
(21) Tsuda, K.; Dol; Gensch, T.; Hofkens, J.; Latterini, L.; Weener; Meijer; De, S. *J. Am. Chem. Soc.* **2000**, *122*, 3445.
(22) Li, S.; McGrath, D. V. *J. Am. Chem. Soc.* **2000**, *122*, 6795.
(23) Junge, D. M.; McGrath, D. V. *J. Am. Chem. Soc.* **1999**, *121*, 4912.
(24) M. Junge, D.; V. McGrath, D. *Chem. Commun.* **1997**, 857.
(25) Buhleier, E.; Wehner, W.; Vögtle, F. *Synthesis* **1978**, 155.
(26) Astruc, D.; Boisselier, E.; Ornelas, C. t. *Chem. Rev.* **2010**, *110*, 1857.
(27) Fréchet, J. M. J.; Tomalia, D. A. *Dendrimers and Other Dendritic Polymers*; John Wiley & Sons, Ltd.: New York, 2001.
(28) Fischer, W.; Calderón, M.; Schulz, A.; Andreou, I.; Weber, M.; Haag, R. *Bioconjugate Chem.* **2010**, *21*, 1744.
(29) Bosman, A. W.; Vestberg, R.; Heumann, A.; Fréchet, J. M. J.; Hawker, C. J. *J. Am. Chem. Soc.* **2002**, *125*, 715.
(30) Killops, K. L.; Campos, L. M.; Hawker, C. J. *J. Am. Chem. Soc.* **2008**, *130*, 5062.
(31) Fischer, W.; Claderon, M.; Ofek, P.; Satchi-Fainaro, R.; Haag, R. *J. Controlled Release* **2010**, *148*, e89.
(32) Calderón, M.; Quadir, M. A.; Strumia, M.; Haag, R. *Biochimie* **2010**, *92*, 1242.
(33) Khan, A.; Daugaard, A. E.; Bayles, A.; Koga, S.; Miki, Y.; Sato, K.; Enda, J.; Hvilsted, S.; Stucky, G. D.; Hawker, C. J. *Chem. Commun.* **2009**, 425.
(34) Elmer, S. L.; Man, S.; Zimmerman, S. C. *Eur. J. Org. Chem.* **2008**, *2008*, 3845.
(35) Jansen, J. F. G. A.; de Brabander-van den Berg, E. M. M.; Meijer, E. W. *Science* **1994**, *266*, 1226.
(36) Li, C.; Wallace, S. *Adv. Drug Deliver. Rev.* **2008**, *60*, 886.
(37) Twaites, B.; de las Heras Alarcon, C.; Alexander, C. *J. Mater. Chem.* **2005**, *15*, 441.
(38) Svenson, S.; Tomalia, D. A. *Adv. Drug Delivery Rev.* **2005**, *57*, 2106.
(39) Gillies, E. R.; Fréchet, J. M. J. *Drug. Discovery Today* **2005**, *10*, 35.
(40) D'Emanuele, A.; Attwood, D. *Adv. Drug Delivery Rev.* **2005**, *57*, 2147.
(41) Duncan, R. *Nat. Rev. Drug Discovery* **2003**, *2*, 347.
(42) Morgenroth, F.; Reuther, E.; Müllen, K. *Angew. Chem., Int. Ed. Engl.* **1997**, *36*, 631.
(43) Morgenroth, F.; Kubel, C.; Mullen, K. *J. Mater. Chem.* **1997**, *7*, 1207.
(44) Grebel-Koehler, D.; Liu, D.; De Feyter, S.; Enkelmann, V.; Weil, T.; Engels, C.; Samyn, C.; Müllen, K.; De Schryver, F. C. *Macromolecules* **2003**, *36*, 578.
(45) van der Poll, D. G.; Kieler-Ferguson, H. M.; Floyd, W. C.; Guillaudeu, S. J.; Jerger, K.; Szoka, F. C.; Fréchet, J. M. *Bioconjugate Chem.* **2010**, *21*, 764.
(46) Morgan, M. T.; Nakanishi, Y.; Kroll, D. J.; Griset, A. P.; Carnahan, M. A.; Wathier, M.; Oberlies, N. H.; Manikumar, G.; Wani, M. C.; Grinstaff, M. W. *Cancer Res.* **2006**, *66*, 11913.
(47) Christie, R. M. *Polym. Int.* **1994**, *34*, 351.
(48) Nagao, Y.; Misono, T. *Dyes Pigm.* **1984**, *5*, 171.
(49) Rademacher, A.; S., M.; Langhals, H. *Chem. Ber.* **1982**, *115*, 2927.
(50) Qu, J.; Pschirer, N. G.; Liu, D.; Stefan, A.; De Schryver, F. C.; Müllen, K. *Chem.—Eur. J.* **2004**, *10*, 528.
(51) Qin, T.; Wiedemair, W.; Nau, S.; Trattnig, R.; Sax, S.; Winkler, S.; Vollmer, A.; Koch, N.; Baumgarten, M.; List, E. J. W.; Müllen, K. *J. Am. Chem. Soc.* **2011**, *133*, 1301.
(52) Flors, C.; Oesterling, I.; Schnitzler, T.; Fron, E.; Schweitzer, G.; Sliwa, M.; Herrmann, A.; van der Auweraer, M.; de Schryver, F. C.; Müllen, K.; Hofkens, J. *J. Phys. Chem. C* **2007**, *111*, 4861.
(53) Cotlet, M.; Vosch, T.; Habuchi, S.; Weil, T.; Müllen, K.; Hofkens, J.; De Schryver, F. *J. Am. Chem. Soc.* **2005**, *127*, 9760.
(54) Métivier, R.; Kulzer, F.; Weil, T.; Müllen, K.; Basché, T. *J. Am. Chem. Soc.* **2004**, *126*, 14364.
(55) Cotlet, M.; Masuo, S.; Luo, G.; Hofkens, J.; Van der Auweraer, M.; Verhoeven, J.; Müllen, K.; Xie, X. S.; De Schryver, F. *Proc. Natl. Acad. Sci. U. S. A.* **2004**, *101*, 14343.
(56) Qu, J.; Liu, D.; De Feyter, S.; Zhang, J.; De Schryver, F. C.; Müllen, K. *J. Org. Chem.* **2003**, *68*, 9802.
(57) Liu, D.; De Feyter, S.; Cotlet, M.; Stefan, A.; Wiesler, U.-M.; Herrmann, A.; Grebel-Koehler, D.; Qu, J.; Müllen, K.; De Schryver, F. C. *Macromolecules* **2003**, *36*, 5918.
(58) Cotlet, M.; Gronheid, R.; Habuchi, S.; Stefan, A.; Barbafina, A.; Müllen, K.; Hofkens, J.; De Schryver, F. C. *J. Am. Chem. Soc.* **2003**, *125*, 13609.
(59) Gronheid, R.; Hofkens, J.; Köhn, F.; Weil, T.; Reuther, E.; Müllen, K.; De Schryver, F. C. *J. Am. Chem. Soc.* **2002**, *124*, 2418.
(60) Weil, T.; Wiesler, U. M.; Herrmann, A.; Bauer, R.; Hofkens, J.; De Schryver, F. C.; Müllen, K. *J. Am. Chem. Soc.* **2001**, *123*, 8101.
(61) Maus, M.; Mitra, S.; Lor, M.; Hofkens, J.; Weil, T.; Herrmann, A.; Müllen, K.; De Schryver, F. C. *J. Phys. Chem. A* **2001**, *105*, 3961.
(62) Maus, M.; De, R.; Lor, M.; Weil, T.; Mitra, S.; Wiesler, U.-M.; Herrmann, A.; Hofkens, J.; Vosch, T.; Müllen, K.; De Schryver, F. C. *J. Am. Chem. Soc.* **2001**, *123*, 7668.
(63) Hofkens, J.; Maus, M.; Gensch, T.; Vosch, T.; Cotlet, M.; Köhn, F.; Herrmann, A.; Müllen, K.; De Schryver, F. *J. Am. Chem. Soc.* **2000**, *122*, 9278.
(64) Devadoss, C.; Bharathi, P.; Moore, J. S. *J. Am. Chem. Soc.* **1996**, *118*, 9635.
(65) Priewisch, B.; Rück-Braun, K. *J. Org. Chem.* **2005**, *70*, 2350.
(66) Shifrina, Z. B.; Rajadurai, M. S.; Firsova, N. V.; Bronstein, L. M.; Huang, X.; Rusanov, A. L.; Muellen, K. *Macromolecules* **2005**, *38*, 9920.
(67) Wang, Y.; Ma, N.; Wang, Z.; Zhang, X. *Angew. Chem., Int. Ed.* **2007**, *46*, 2823.
(68) The solution of **1** did not entirely return to its initial state after being exposed to 450 nm. This can be explained by the overlap absorption spectra of cis and trans isomer at 450 nm. However, 100% recovery of *trans*-AB was observed after keeping the irradiated solution in the dark within a few hours.

(69) First, the initial solution of dendrimer **1** (without any irradiation) was exposed to 450 nm light for 2 min, so that the solution can reach the photostationary state at 450 nm (PSS 450 nm, solid red line shown in Figure 4). At this state, the absorbance value at 370 nm was used as a reference for 10 switching experiments.

(70) SEC elution volumes were converted to hydrodynamic volume values by use of the relationship $V_h = 0.4(KM^{a+1})$, as described (*J. Am. Chem. Soc.* **2004**, *126*, 2183), where K and a are the Mark−Houwing constants for polystyrene in THF and M is the coeluting polystyrene molecular weight.

(71) There is a difference in changes of hydrodynamic volume of dendrimer **1** (before and after irradiation) detected by SEC and FCS, because in an FCS experiment, the irradiated solution can be measured immediately after being exposed to 365 nm (trans to cis), while in a SEC experiment, the irradiated solution needs to be passed through a long GPC column before being detected (for more details, see Supporting Information Figure 9)

(72) A 5.4×10^{-4} M solution of **1** in CD_2Cl_2 was irradiated at 365 nm for 60 min. The longer irradiation time compared to previous UV studies was necessary due to the much higher concentration of the solution used for the NMR experiment. The achievement of a PSS was checked by UV−vis spectroscopy prior to the NMR experiment.

(73) Ramsteiner, I. B.; Hartschuh, A.; Port, H. *Chem. Phys. Lett.* **2001**, *343*, 83.

(74) Seibold, M.; Port, H.; Wolf, H. C. *Mol. Cryst. Liq. Cryst.* **1996**, *283*, 75.

(75) Irie, M.; Fukaminato, T.; Sasaki, T.; Tamai, N.; Kawai, T. *Nature* **2002**, *420*, 759.

(76) Feng, Y.; Feng, W. *Opt. Mater.* **2008**, *30*, 876.

(77) To a 5.4×10^{-4} M solution of **1** in CD_2Cl_2 were added precise amounts of guest molecules (0.1 M solution in CD_2Cl_2) successively. After each addition, the ^{1}H NMR spectrum of the mixture was recorded. Due to the relatively high concentration of guest solution, the volume change upon guest addition is negligible.

(78) A value of two guest molecules per dendrimer was obtained when a mixture (3 mL) of the dendritic host **1** (0.25 M, 1 equiv) and guest molecules *p*-NP (5 M, 20 equiv) was used. When using less than 20 equiv of guest, the result is not reproducible; i.e, sometimes 2 equiv and sometimes 1 equiv of guests per dendrimer was observed. Upon using more guests (from 20−1000 equiv), all the experiments gave reproducible results, i.e, 2.5 equiv of guests per dendrimer.